

## Self-affinity of time series with finite domain power-law power spectrum

Oleg I. Yordanov and Nickolay I. Nickolaev

*Institute of Electronics, Boulevard Tzarigradsko chaussée 72, Sofia 1784, Bulgaria*

(Received 27 May 1993)

We consider time series with finite domain (band-limited) power-law spectra. Our analysis is based on exact representation of the structure (mean square increment) function for such processes and shows that the considered time series exhibit an approximate self-affinity in a wide range of time scales. The self-affinity is embodied in the leading asymptotic term which represents the familiar "pure" fractal behavior. Next we explicitly show that the impact of the lowest and the highest scales of the process cannot in general be neglected and conclude from this that for adequate description of the natural processes considerations beyond the simple fractal analysis are required. We also propose a method for determining the spectral parameters of experimentally recorded self-affine time series which is based on nonlinear, least-squares fit and the exact form of the structure function. Tests employing numerically generated series as a benchmark demonstrate this method's excellent accuracy and robustness.

PACS number(s): 05.40.+j, 02.50.Ey, 02.60.Ed

Random processes with power-law frequency spectra,  $S(f) = Af^{-\alpha}$ , provide apt descriptions for a variety of complex structures and physical phenomena. An incomplete list of applications includes terrestrial and man-made rough surfaces [1], fracture surfaces [2], the ocean bottom [3], the surface of the Moon [4], the structure of the atmospheric turbulence [5,6], ocean waves' spectra under various sea and atmospheric conditions [7,8], fractional Brownian motion and fractional (colored) noises [9], etc. Power-law type behavior has also been identified in biological systems [10] and as short trends, even in stock-market fluctuations [11]. It is therefore of prime interest to develop more precise and reliable methods for retrieving the parameters of the spectra from experimentally recorded time series [12].

Modern approaches utilize for this purpose self-similar [9,13] or in general, self-affine [14] properties of the power-law processes. For a given random time series  $x(t)$  these properties can be illustrated by considering its structure function (SF) defined by [6]  $\Delta(t_1, t_2) = \langle [x(t_1) - x(t_2)]^2 \rangle$ ; the angle brackets designate ensemble average. More specifically, it has been shown [13] that for a Gaussian random process, having a power-law spectrum with no characteristic scales:  $\Delta(\alpha, \tau) \propto \tau^{\alpha-1}$ , where  $\tau = |t_1 - t_2|$ . [Often, the notation  $H = (\alpha - 1)/2$  is alternatively used;  $H$  is called Hurst's exponent [15]]. Thus, for every real  $\rho > 0$ ,  $x(\rho t)$  and  $\rho^{(\alpha-1)/2}x(t)$  have identical structure functions and therefore are statistically indistinguishable. Further, the graphs of the  $x(t)$  realizations are fractals with fractal (Hausdorff) dimension  $D$  which is solely related to the spectral exponent [16,13]

$$D = (5 - \alpha)/2. \quad (1)$$

Several algorithms for estimating the fractal dimension have recently been tested using as a benchmark numerically generated power-law time series with prescribed  $\alpha$  [17-20]. Compared to the spectral methods these algo-

gorithms render superior estimates of  $\alpha$  [through Eq. (1)]; see in particular Ref. [17], where this comparison is explicitly carried out. And yet, certain systematic deviations from the linear relationship between the power-law index and the fractal dimension (1) are reported in all numerical experiments. More precisely, for  $\alpha > 2$  (or equivalently  $D < 1.5$ ), Eq. (1) underestimates the calculated fractal dimension; conversely, for  $\alpha < 2$  ( $D > 1.5$ ) Eq. (1) overestimates the calculated fractal dimension. These discrepancies are more pronounced when  $D \rightarrow 1$  and  $D \rightarrow 2$ , important special cases referred to as marginal and extreme fractals, respectively [13].

To understand why these discrepancies occur we remark that (1) has been derived for a power-law process with no characteristic scales, i.e., for processes that are pure fractals [13]. Any real process, however, has both a smallest and largest physical scale which imposes in the frequency domain a high and a low frequency cutoff, respectively. Implicit cutoffs, implied by the finite length and the discretization step, do exist for the numerically generated time series as well. It has been conjectured [18] on the basis of extensive numerical simulations that the discrepancies can be explained if the impact of the frequency cutoffs is accounted for; see also [21]. This task appears not to have been carried out and it will be our first concern in this paper. The second will be the introduction of an algorithm for retrieving all (not only  $\alpha$ ) parameters of a finite domain power-law spectra. The last, but perhaps conceptually most important aim, is to demonstrate, on the particular example of self-affine processes of the type considered here, that methods based on scaling properties, as informative as they can be, are fundamentally limited and provide only an approximate description of the natural phenomena.

For the above purposes we consider random processes having power-law spectra with sharp spectral cutoffs  $f_1$  and  $f_2$ , i.e.,  $S(f) = 0$  for  $f < f_1$ ,  $f > f_2$ . Our analysis is straightforward and begins with the remark that the SF of such processes can be represented in the following *exact* form:

$$\Delta(\alpha, \tau) = \Delta_1(\alpha, \tau) - \Delta_2(\alpha, \tau), \quad (2)$$

where  $\Delta_i$ ,  $i = 1, 2$ , are functions expressed in terms of the type (1,2) hypergeometric function

$$\Delta_i(\alpha, \tau) = 2\sigma_i^2 \left[ 1 - {}_1F_2 \left( \frac{1-\alpha}{2}; \frac{3-\alpha}{2}, \frac{1}{2}; -(\pi f_i \tau)^2 \right) \right]$$

and  $\sigma_i^2 = Af_i^{1-\alpha}/(\alpha - 1)$ . The variance of  $x(t)$  is  $\sigma^2 = \langle x^2(t) \rangle = \sigma_1^2 - \sigma_2^2$ . An expression for the SF corresponding to spectra with a low-frequency cutoff only is given in Ref. [22]. Formula (2) easily follows from the spectral representation [6] of  $\Delta(\alpha, \tau)$  by expanding the cosine term in this representation and integrating term-by-term. It is valid for arbitrary time lag  $\tau$ , provided  $\alpha \neq 2n + 1$ ,  $n = 0, 1, 2, \dots$ . In what follows, however, we shall restrict our analysis to the interval  $\alpha \in (1, 3)$ , for which  $x(t)$  is (approximately as we shall see in a moment) self-affine. (The analysis of the power-law spectra with values of the spectral exponent  $\alpha > 3$  and  $\alpha = 2n + 1$  will be presented in a forthcoming paper.)

Self-affinity is not apparent from Eq. (2) and in fact as defined  $x(t)$  does not exhibit exact self-affinity. To see how an approximate self-affinity comes forward, we note that in the natural models most often  $f_2 \gg f_1$ , in which case for  $\tau \gg (2\pi f_2)^{-1}$ ,  $\Delta_2$  is more adequately represented by its full asymptotic expansion. Accordingly,

$$\Delta(\alpha, \tau) = \chi^{3-\alpha} \tau^{\alpha-1} + \Delta_1(\alpha, \tau) - 2\sigma_2^2 \times \left[ 1 + \sum_{k=1}^{\infty} (-1)^k (\alpha - 1)_k \frac{\cos(2\pi f_2 \tau + k\pi/2)}{(2\pi f_2 \tau)^k} \right]. \quad (3)$$

In (3),  $(a)_k = \Gamma(a+k)/\Gamma(a)$  is the Pochhammer's symbol,  $\Gamma$  is the gamma function, and

$$\chi^{3-\alpha} = 2A \frac{\pi^{\alpha-1/2} \Gamma[(3-\alpha)/2]}{\alpha-1 \Gamma(\alpha/2)} \quad (4)$$

is a quantity similar in expression to topothesy introduced in Ref. [13] to describe the topography of rough surfaces. The physical dimension of  $\chi$  is  $[\text{dim } x]^{2/(3-\alpha)} \times [\text{time}]^{(1-\alpha)/(3-\alpha)}$ ; note that  $\chi$  does not depend on  $f_1$  and  $f_2$ .

The SF in the pure fractal case is represented only by the first term in (3) for all time intervals. The oscillations produced by the third term, involving  $f_2$ , are noticeable only for processes with relatively large  $\sigma_2^2$ ; i.e., for processes close to the extreme fractal case, see also Fig. 1 below and the related comments. With increasing  $\tau$  the magnitude of these oscillations decreases. For small values of its argument  ${}_1F_2 \approx 1$  and therefore it is the first term that is dominant in (3) for  $(2\pi f_2)^{-1} \ll \tau \ll (2\pi f_1)^{-1}$  rendering the approximate self-affinity. For longer times the effect of the second term in (3) increases and if  $\tau \gg (2\pi f_1)^{-1}$  the SF enters its second asymptotic regime in which it approaches  $2\sigma^2$  in an oscillatory manner:

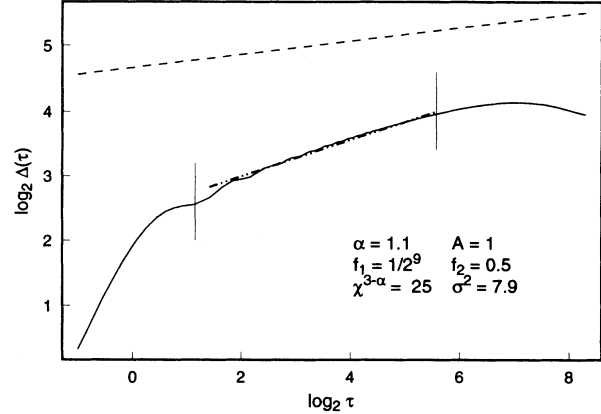


FIG. 1. Log-log graph of the structure function of a random process with finite domain power-law spectrum (solid curve). The parameters of the spectrum, the variance  $\sigma^2$  and  $\chi$  [see Eq. (4)] are given in the legend. The dashed-dotted line represents the best linear fit to  $\log_2 \Delta(\alpha, \tau)$  within the self-affinity interval. The positions of the crossover times are marked by vertical lines. The corresponding pure fractal process is illustrated by the dashed line.

$$\Delta(\alpha, \tau) \approx 2\sigma^2 + 2\sigma_1^2 \sum_{k=1}^{\infty} (-1)^k (\alpha - 1)_k \times \frac{\cos(2\pi f_1 \tau + k\pi/2)}{(2\pi f_1 \tau)^k}. \quad (5)$$

A trigonometric series involving inverse powers of  $f_2$ , see (3), is neglected in (5).

The end points of the time interval in which  $x(t)$  displays approximate self-affinity (crossover times) can roughly be estimated by equating the leading order terms representing  $\Delta(\alpha, \tau)$  for short and intermediate, and intermediate and long times [21]. From Eqs. (2) and (3) for the first crossover time we infer

$$\tau_1 = \left[ \frac{\sqrt{\pi}}{(\alpha - 1)} \frac{\Gamma((5 - \alpha)/2)}{\Gamma(\alpha/2)} \right]^{1/(3-\alpha)} \frac{1}{\pi f_2} \quad (6)$$

and from (3) and (5) we have

$$\tau_2 = \left[ \frac{\Gamma(\alpha/2)}{\sqrt{\pi} \Gamma((3 - \alpha)/2)} \right]^{1/(\alpha-1)} \frac{1}{\pi f_1}. \quad (7)$$

The time interval  $(\tau_1, \tau_2)$  is called scaling or self-affinity interval.

Graphs of  $\log_2 \Delta(\alpha, \tau)$  versus  $\log_2 \tau$  are shown in Fig. 1 (solid curve) for  $\alpha = 1.1$  and in Fig. 2 for  $\alpha = 2.8$ ; the other spectral parameters used to draw the graphs are given in the legends. In addition, the SF's for the corresponding pure fractal case are illustrated by dashed lines. (It is worth noting at this moment that the processes considered here are not true fractals [23], for their Hausdorff-Besicovitch dimension is  $D = 1$ . One can show this by repeating the steps of Orey's proof [16] and reckoning with the behavior of (2) as  $\tau \rightarrow 0$ . Thus, at very fine resolutions the graphs of  $x(t)$  realizations are rectifiable [24] curves.) The dashed-dotted lines represent the best linear fit to  $\log_2 \Delta(\alpha, \tau)$  within their respective intervals of self-affinity. If one adheres to the pure frac-

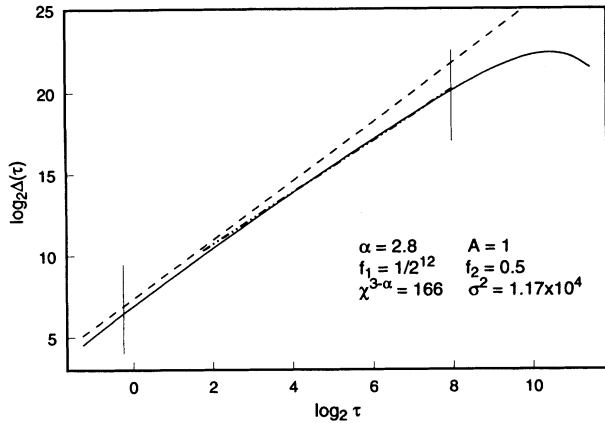


FIG. 2. The same as Fig. 1 but for different spectral parameters.

tal concept, the slope of these lines should be  $2H$ . From Fig. 1,  $H = 0.141$ , thus the estimated fractal dimension is  $D_{est} = 2 - H = 1.859$ , well below that following from Eq. (1):  $D = 1.95$ . Conversely, from Fig. 2,  $D_{est} = 1.21$  which is higher than the expected value of  $D = 1.1$ .

Equation (3) shows that these systematic deviations are due to the influence which the spectral cutoffs have on the behavior of the SF in the scaling interval. Indeed, the third term in (3), respectively the upper cutoff, affects the values of  $\Delta(\alpha, \tau)$  only for times relatively close to  $\tau_1$  as the magnitude of this correction is significant only when  $\alpha < 2$  and increases for  $\alpha \rightarrow 1$ . Conversely, the lower cutoff affects  $\Delta(\alpha, \tau)$  for  $\tau$  close to  $\tau_2$  and  $\alpha > 2$ . The imbalance between the second and the third terms in (3) alters the tilt of the SF (when compared to the pure fractal case) and causes the systematic deviations observed in the numerical experiments. With decreasing the ratio  $\delta = f_1/f_2$  the deviations decrease with a rate which can be quantified by considering the slope of the SF at the middle point for the interval  $(\log_2 \tau_1, \log_2 \tau_2)$ . From Eq. (3), accounting for the leading orders in  $\delta$  only, this slope is given by the ratio

$$s(\alpha) \approx \frac{(\alpha - 1) - 2p^{1/(\alpha-1)}\delta^{(3-\alpha)/2}}{1 - p^{1/(\alpha-1)}\delta^{(3-\alpha)/2} - p^{1/(3-\alpha)}\delta^{(\alpha-1)/2}}, \quad (8)$$

where

$$p = (\alpha - 1)^{(\alpha-1)/2} \left(\frac{3 - \alpha}{2}\right)^{(3-\alpha)/2} \frac{\Gamma(\alpha/2)}{\sqrt{\pi}\Gamma((5 - \alpha)/2)}.$$

We recall that in the majority of the applications  $\delta \ll 1$ . Hence, if  $\alpha \gtrsim 1$ , only the last term in the denominator is not negligible which leads to a slope greater than that corresponding to the fractal case:  $s_f = \alpha - 1$ . With increasing  $\alpha$ ,  $s(\alpha)$  approaches  $s_f$  until  $\alpha$  reaches 2, where according to (8),  $s(2) = s_f(2) = 1$ . Further increase of  $\alpha$  increases the importance of the second terms in both the numerator and denominator, and in effect  $s < s_f$  for  $2 < \alpha < 3$ . In terms of the relative deviation  $(D_{est} - D)/D$ , where  $D_{est} = 2 - s(\alpha)/2$  and  $D$  is given by Eq. (1), this behavior of  $s$  translates into negative values for  $\alpha < 2$ , zero for  $\alpha = 2$ , and positive values of relative

deviations for  $\alpha > 2$ . Equation (8) correctly predicts relative deviations whose magnitudes for  $\alpha \lesssim 3$  are greater than those for  $\alpha \gtrsim 1$ . The latter has previously been found in the numerical simulations; see Fig. 5 in [20].

It is interesting to specify the range of  $\delta$  values in which for a given  $\alpha$  the random process is close to the corresponding pure fractal process. Let either  $\alpha = 1 + \varepsilon$  or  $\alpha = 3 - \varepsilon$  with  $\varepsilon$  fixed;  $0 < \varepsilon < 1$ . From (8), the corrections to  $s_f$  are less than, say 1%, provided  $\delta < 10^{-4}/\varepsilon$ . Thus, for small  $\varepsilon$  the convergence of the finite domain power-law process towards its idealized fractal analog is extremely slow, a fact also confirmed by the numerical simulations [20].

The fact that the harmonics outside the power-law region of the spectrum, or their lack, can affect and alter the overall (fractal) behavior leads to an important conclusion: namely, when a real process or structure that appears self-affine is encountered, attempts to either justify the use of the simple fractal models or more often attempts to improve them by including terms beyond the leading order have to be carried out.

The analysis hitherto of a band-limited, power-law process implies a straightforward method for retrieving the spectral parameters of experimentally recorded time series: that is, calculate the SF associated with the time series for various time lags and fit these data with the expressions (2), (3), and (5) in their respective intervals of validity using a nonlinear, least-square algorithm. In addition to the advantage of being based on exact results, such an approach renders all spectral parameters and removes the necessity for selecting the interval of self-affinity which often is an ambiguous step. We remark also that  ${}_1F_2$  is an entire function (numerically converging faster than the exponential function from the same argument); the asymptotic series in (3) and (5) are easily summed using the optimal truncation rule [25]; intervals of validity of (2) and (3) from one side, and (3) and (5) from the other overlap in which cases these expressions yield identical values. The latter considerably facilitates the implementation of the fitting procedure and makes it efficient.

The method has been tested versus numerically generated time series [18,26] with preselected spectral parameters. For this purpose we use uniformly distributed, approximately  $\delta$ -function correlated phases in the interval  $[0, 2\pi]$ . The total length of the time series is  $2^{13}$ ; the discretization interval for all runs is  $\Delta t = 1$  which leads to an upper cutoff of  $f_2 = 0.5$ . The lower cutoffs are explicitly imposed for any particular realization. The structure function for a given realization is calculated using a method similar to that presented by Higuchi [17] appropriately modified so as to yield the mean square increment of the time series instead of its average "length." An accuracy of at least  $10^{-6}$  has been required and achieved from the nonlinear least-square fit. Typical results are presented in Table I, where the retrieved parameters for three sets of time series characterized by different  $\alpha$  are given. An excellent agreement with the spectral parameters used for the time series generation (see the caption of the table) has been obtained in these as well as other runs which we have carried out but are

not presented here.

It is a good strategy to use the outcome from either the spectral or fractal methods as starting values for the nonlinear fit. However, all numerical experiments conducted by us indicate that the procedure converges to the true spectral values even when the initial values are chosen distantly apart. For example, the starting values for the runs presented in Table I are  $f_1 = 0.01$ ,  $f_2 = 0.1$ ,  $A = 5.0$ , and  $\alpha = 2.0$  (the first and the third sets),  $\alpha = 1.5$  (the second set). We remark that the method is not limited to the case  $f_1 \ll f_2$  and thus it is uniquely suitable for identification of relatively short time, approximate self-affine trends, and also for processing a limited number of experimental data. The accuracy and the robustness of the method suggest that a simple modification may prove useful in cases when more complicated spectra, characterized by several different spectral exponents in different frequency intervals, are involved. The SF for such spectra can be constructed as a sum of several functions of type (2). Although usually sharp, the cutoffs of the realistic power-law spectra are not absolutely sharp. We note, however, that the contribution to the SF of the spectral regions in which the cutoffs effectively take place is additive. Therefore the expressions obtained here constitute the essential part of any realistic self-affine SF. Finally, we expect that the knowledge of the precise form of the SF for finite domain power-law

TABLE I. Retrieved spectral parameters for time series generated by using  $\alpha = 1.2$  (upper part of the table),  $\alpha = 2.0$  (middle part), and  $\alpha = 2.8$  (lower part); in all parts the first row corresponds to  $f_1 = 1/2^8$ , second to  $f_1 = 1/2^9$ , and the third to  $f_1 = 1/2^{10}$ ; in all examples  $A = 1$  and  $f_2 = 0.5$ .

$\alpha$	$A$	$f_1$	$f_2$
1.2010	0.9981	$0.3828 \times 10^{-2}$	0.5001
1.2008	0.9984	$0.1828 \times 10^{-2}$	0.5000
1.2008	0.9985	$0.9165 \times 10^{-3}$	0.5000
2.0009	0.9976	$0.3836 \times 10^{-2}$	0.5004
2.0006	0.9984	$0.1869 \times 10^{-2}$	0.5002
2.0005	0.9988	$0.1007 \times 10^{-2}$	0.5001
2.8012	0.9959	$0.3842 \times 10^{-2}$	0.5017
2.8005	0.9976	$0.1882 \times 10^{-2}$	0.5010
2.8000	0.9990	$0.1025 \times 10^{-2}$	0.5004

spectra will be useful for distinguishing between empirical time series that result from low-dimensional strange attractors and those from stochastic processes [27].

We acknowledge support by the Bulgarian Ministry of Science and Education, Grant No. F4. One of us (O.I.Y.) would like to thank G. L. Hower and S. L. Broschat for their hospitality at the School of Electrical Engineering and Computer Science, Washington State University, where part of this work was completed.

- [1] R. S. Sayles and T. R. Thomas, *Nature (London)* **271**, 431 (1978); M. V. Berry and J. R. Hannay, *ibid.* **273**, 573 (1978); B. Klinkenberg and M. F. Goodchild, *Earth Surface Processes and Landforms* **17**, 217 (1992).
- [2] B. B. Mandelbrot, D. E. Passoja, and A. J. Paullay, *Nature (London)* **308**, 721 (1984); Ma Zhenyi *et al.*, *J. Mater. Res.* **6**, 183 (1991).
- [3] T. H. Bell, Jr., *Deep-Sea Res.* **26A**, 65 (1978).
- [4] I. M. Fuks, *Radiophys. Quantum Electron.* **26**, 865 (1983).
- [5] A. N. Kolmogorov, *C.R. Acad. Sci. USSR* **30**, 299 (1941); S. Chen *et al.*, *Phys. Fluids A* **5**, 458 (1993).
- [6] S. Panchev, *Random Functions and Turbulence* (Pergamon Press, Oxford, 1971); A. S. Monin and A. M. Yaglom, *Statistical Fluid Mechanics* (MIT Press, Boston, 1971).
- [7] O. M. Phillips, *J. Fluid Mech.* **4**, 226 (1958); V. E. Zakharov and N. N. Filonenko, *J. Appl. Mech. Tech. Phys.* **8**, 62 (1967).
- [8] W. J. Pierson, Jr. and L. Moskowitz, *J. Geophys. Res.* **69**, 5181 (1964); S. Elgar and G. Mayer-Kress, *Physica D* **37**, 104 (1989); M. Y. Stiassnie *et al.*, *ibid.* **47**, 341 (1991).
- [9] B. B. Mandelbrot and J. W. van Ness, *SIAM (Soc. Ind. Appl. Math.) Rev.* **10**, 422 (1968); J. Llosa and J. Masoliver, *Phys. Rev. A* **42**, 5011 (1990).
- [10] R. F. Voss, *Phys. Rev. Lett.* **68**, 3805 (1992); H. E. Stanley, *Physica A* **186**, 1, 1992.
- [11] M. R. Schroder, *Fractals, Chaos, Power Laws* (W. H. Freeman Company, New York, 1991), p. 222.
- [12] P. G. Drazin and G. P. King, *Physica D* **58**, vii (1992).
- [13] M. V. Berry, *J. Phys. A: Math. Gen.* **12**, 781 (1979).
- [14] B. B. Mandelbrot, *Phys. Scr.* **32**, 257 (1985); B. B. Mandelbrot, in *Fractals in Physics*, edited by L. Pietronero and E. Tosatti (North-Holland, Amsterdam, 1986).
- [15] B. B. Mandelbrot, *The Fractal Geometry of Nature* (Freeman, San Francisco, 1982).
- [16] S. Orey, *Z. Wahrsch'theorie verw. Geb.* **15**, 249 (1970).
- [17] T. Higuchi, *Physica D* **31**, 277 (1988).
- [18] A. R. Osborne and A. Provenzale, *Physica D* **35**, 357 (1989).
- [19] T. Higuchi, *Physica D* **46**, 254 (1990).
- [20] N. P. Greis and H. S. Greenside, *Phys. Rev. A* **44**, 2324 (1991).
- [21] J. Theiler, *Phys. Lett. A* **155**, 480 (1991).
- [22] O. I. Yordanov, in *Huygens' Principle 1690-1990: Theory and Applications*, edited by H. Blok, H. A. Ferwerda, and H. K. Kuiken, *Studies in Mathematical Physics Vol. 3* (Elsevier, Amsterdam, 1992), p. 559.
- [23] According to Mandelbrot's tentative definition, see Ref. [15], page 361.
- [24] K. J. Falconer, *The Geometry of Fractal Sets* (Cambridge University Press, Cambridge, England, 1985).
- [25] C. M. Bender and S. A. Orszag, *Advanced Mathematical Methods for Scientists and Engineers* (McGraw-Hill, New York, 1978).
- [26] K. Y. R. Billah and M. Shinozuka, *Phys. Rev. A* **42**, 7492 (1990).
- [27] P. Grassberger, *Nature (London)* **323**, 609 (1986); I. Procaccia, *ibid.* **333**, 498 (1988); D. T. Kaplan and L. Glass, *Phys. Rev. Lett.* **68**, 427 (1992); A. Provenzale *et al.*, *Physica D* **58**, 31 (1992).